BioNanoScience (2022) 12:540–554
https://doi.org/10.1007/s12668-022-00964-4

Nanoemulsions (O/W) containing *Cymbopogon pendulus* essential oil: development, characterization, stability study, and evaluation of in vitro anti-bacterial, anti-inflammatory, anti-diabetic activities

Suraj Agnish[1] · Arun Dev Sharma[1] · Inderjeet Kaur[1]

Accepted: 24 February 2022 / Published online: 2 March 2022

Abstract
Essential oil from *Cymbopogon pendulus* is immensely useful in various sectors like food, pharmaceutical, and cosmetic industries. Since this oil is hydrophobic, unstable, and volatile, hence encapsulation by using nanoemulsions technology is the best way to protect it. This study reports biosynthesis of O/W (oil/water) nanoemulsions based on essential oil from *Cymbopogon pendulus* and analysis of its biological activities. O/W nanoemulsions were prepared by using tween 20/80, sodium dodecyl sulphate as surfactants, and ethanol as co-surfactants. Fingerprinting of nanoemulsions using UV, fluorescent, and FT-IR was studied along with other parameters like pH and conductivity. Biological activities like antibacterial, anti-inflammatory, and anti-diabetic activities and drug release pharmokinetics were evaluated. Ethanol containing nanoemulsions was noticeably smaller than other nanoemulsions. Encapsulation efficiency of nanoemulsions was in the range from 41 to 60%. Nanoemulsions were spherical in shape and stable even after 50 days of storage. Appreciable biological activities like anti-bacterial, anti-inflammatory, and anti-diabetic activities were detected. Drug kinetic study revealed that nanoemulsions exhibited Korsmeyer-Peppas model. Based on this, the possible role of lemon grass oil-based nanoemulsions in cosmetic, food, and pharma sectors has been discussed.

Keywords Nanoemulsion · *Cymbopogon pendulus* oil · Tween 20 · Ethanol · Antimicrobial activity

1 Introduction

Day by day the role of plants-based secondary metabolites is increasing worldwide. Among all secondary metabolites, plant-based essential oils which represent "green technology" hold central place in pharma- and food-based industries due to various biological activities like: anti-bacterial, anti-viral, and insecticidal. Plant-based essential oils contain a mixture of different major and minor bio-active molecules such as phenolics, flavonoids, esters, aldehydes, terpenes, and alcohols [1]. By owing to such diverse bioactives, with time a lot of interest for essential oils has been generated among researchers [2].

Essential oil from *Cymbopogon pendulus* (also known as lemon grass oil, LGO), poaceae family, is widely used as traditional medicine worldwide as complementary and alternative medicine [2]. Lemon grass essential oil extracted from their leaves is rich in many bioactive compounds that extensively contribute to its antioxidant and phytomedicinal properties. LGO contains many bioactives like linalool, geraniol, citronellol, nerol, 1, 8-cineole, citronellal, β-pine, β-thujene, β-carophyllene oxide, geranial acetate, methyl heptane, dipentene, alpha pinene, and terpenolene [3]. Literature studies reveal citral to be the major constituent (65–85%) of lemongrass essential oil which is found as a mixture of two monoterpene stereoisomer namely, Citral-A (Trans isomer or Geranial) and Citral-B (Cis isomer or Neral) [4]. Citral is used as an important component in manufacturing of perfumes, cosmetics, food and pharmaceutical products. However, its degradation produces off-flavor compounds. Despite of these pharmacological and biological importances, LGO is found to be unstable on prolonged storage at room temperature. It is also highly susceptible to oxidative degradation, and is sparingly soluble in water [5]. These disadvantages lead to decrease in biochemical and pharmacological activities of lemongrass essential oil.

✉ Arun Dev Sharma
arundevsharma47@gmail.com

[1] PG Dept. of Biotechnology, Lyallpur Khalsa College, Jalandhar, Punjab, India

In order to improve, stability, utilization, and efficiency of essential oils, during recent times, encapsulation of oils which represent thermo-dynamically and kinetically stable dispersions has been selected as a key technique [6]. The nanoemulsions pose tendency to encapsulate bioactive molecules including antioxidants and phytobioactive ingredients. The food-based industries these nanoemulsions are used for controlled release of flavor compounds in foods [7]. In addition, nanoemulsions-based edible nano-coating of coloring and flavor bioactives, anti-browning agents, antioxidants, and anti-microbials are used to coat much foods stuff like meat, dairy products like cheese, fresh fruits, vegetables, and other confectionary items just to enhance their shelf life. These nanoemulsions minimize moisture loss, gas exchange, and oxidation of food items [8]. It was cited that encapsulation of bioactives in form of nanoemulsions increase its stability, solubility, regulated release and enhance absorption in the gastrointestinal tract, and through cells [9]. The nano-emulsions act as carrier molecules with high affinity to target site for those drugs which are otherwise susceptible to biological degradation or required in large concentrations in human body [9].

During recently, nanoemulsions technology has gained tremendous importance in various stakeholders like cosmetic, food, and phama-based companies as [10]. Broadly, nanoemulsions can be categorized as water-in-oil (W/O) and oil-in-water (O/W) [11]. This type of emulsions poses capability to effectively deliver aroma and flavors based hydrophobic herbal derivatives with enhanced surface area, bioavailability and absorption rate. By this way hydrophobic bio active molecules can be incorporated into oil phase of nanoemulsions with the help of surfactants and co-surfactant like Tween 20/80, SDS and ethanol etc. [12, 13]. As LGO from *Cymbopogon pendulus* is widely used in cosmetic, food, and phama-based industries, however, encapsulation based nanoemulsions studies have received considerably much less attention. Hence, the objective of this study was biosynthesis of lemon grass oil-based nanoemulsions and its evaluation of biological activities.

2 Material and methods

2.1 Essential oil extraction

Leaves of *Cymbopogon pendulus* were collected from campus fields and plots. Plants were verified by Dr Upma from Botany department. Lemon grass oil from leaves of was extracted by using Steam-distillation method as described in Sharma et al. [14]. Oil obtained was stored in dark bottles at 4 °C till further use.

2.2 Preparation of nanoemulsions

Cymbopogon pendulus essential oil-based nanoemulsions were synthesized as described in Sharma et al. [15] by some modifications. Briefly, six nanoemulsion formulations (F1–F6) were prepared (Supplementary Table 1). For F1 and F2, Tween 20 and Tween 80, respectively, (2v/v%) solution was prepared in water and shaken for 10 min. For making F3-F4, SDS (0.30 w/w%) was added to F1 and F2 and shaken for 10 min. F5 and F6 were prepared by adding ethanol (25%) to F1 and F2 nano-formulations and shaken for 10 min. Drop wise lemon grass oil (5 v/v%) was added to all formulations with constant shaking with magnetic stirrer at 2000 rpm for 30 min and further subjected to sonication by using high frequency ultrasonicator (Citizen, CDT, UC-2000) at 25 kHz frequency for 15 min at 20 °C.

2.3 Physiochemical studies

All nanoemulsions F1-F6 were observed with the help of microscope and analyzed by in-built MicroView tool (Debro DM RL) as described in Sharma et al. (2021). Nanoemulsions were further evaluated by taking % % transmittance and turbidity at OD at 600 nm by UV–VIS spectrophotometer (Labtronics). pH and conductivity of prepared emulsions were also measured by using pH meter (Labtronics) and conductometer (Labtronics) at room temperature. Dilution test was performed by taking 1 mL of nanoemulsions (F1–F6) in 10 mL of H_2O noticed for phase inversion. Dye solubility (o/w test) test was performed by taking diluted mehylene blue dye which was added to 2.0 mL of nanoemulsions, mixed and noticed for phase inversion with the help of microscope.

2.4 Drug entrapment efficiency (DIE)

DIE of formulated nanoemulsions was carried out by taking 2.0 mL of nanoemulsions, 6 mL of methanol was added and shaken for 20 min at 50 rpm, 37 °C and analyzed at 210 nm using UV spectrometer. The non-incorporated essential oil which was present in aqueous phase was also measured. Drug entrapment efficiency (DEE%) = [total essential oil concentration—free essential oil concentration/ theoretical essential oil concentration] × 100.

2.5 Stability of nanoemulsions

Storage stability of nanoemulsions was studied by storing nanoformulations at RT, 20 °C 4 °C, for 50 days and droplet size was observed.

2.6 Drug kinetics

Drug release kinetics under in vitro conditions using the dialysis technique was studied as described previously [15]. Briefly, in a dialysis bag, 3 mL of F5 and F6 nano-formulations was (holding approximately 1500 mg of oil) was blended with PBS (MW 1000, Sigma). Dialysis was tightly tagged and suspended in a glass beaker having 70 ml of PBS at 37 °C with constant stirring (150 rpm) and at regular intervals about 6 mL of aliquot was taken and studied at 215 nm by UV-spectrophotometer.Total dissolution volume was maintained by adding fresh PBS solutions. Drug release under in vitro conditions was articulated as % essential oil release. Kinetics of drug release was studied by using four models: zero order, 1st order, Korsmeyer-Peppas model and Higuchi model as stated in Sharma et al. [15] (Supplementary table 2).

2.7 Fluorescence, FT-IR, UV–VIS analysis

Characterization of F1 to F6 nanoemulsions were studied by UV-spectrophotometric analysis, FT-IR analysis, and fluorescence emission spectrum analysis following Sharma et a [14, 15].

2.8 Anti-inflammatory activity (protein denaturation)

Tryptophan fluorescent spectroscopy analysis was used for protein denaturation assay (Sharma et al. [14, 15]. For this reaction mixture was prepared having 0.5 mL 1.5% BSA, 6.0 mL of PBS (pH 6.4) and F5 and F5 nanoemulsions. After that tubes having all components were kept at 37 °C for 20 min followed by heating at 70 °C for 7 min and mixture was immediately cool down. Two milliliters of mixture was studied by fluorescent spectroscopy analysis (excitation wavelength 280 nm) on Perkin Elmer Spectrophotometer (FL6500).

2.9 Alpha amylase inhibition (anti-diabetic) assay

Different aliquots of F1–F6 (50–250 µl) was placed in a tube and 125 µl of 0.02 M sodium phosphate buffer (pH 6.9) having α-amylase solution (5 mg/ml) was added. 500 µl of 0.02 M sodium phosphate buffer (pH 6.9) was mixed and solution was incubated at 25 °C for 20 min. Then 600 µl of 2% of starch solution (in 0.03 M sodium phosphate buffer, pH 6.9) was mixed and incubated further at 26 °C for 15 min. 500 µl of dinitrosalicyclic acid was added to stop the reaction. Then tubes were incubated at 100 °C for 10 min and cooled. 6 ml of water added and absorbance was measured at 540 nm. The α-amylase inhibitor activity was calculated as follows: % Inhibition = $Abs_{control} - Abs_{sample} \times 100 / Abs_{control}$. For control, sample was replaced with water.

2.10 Mode of alpha-amylase inhibition

Mode of α-amylase inhibition by F5 and F6 nanoemulsions was conducted as follows. Seventy-five microliters of nanoemulsions was pre-incubated with 200 µl of α-amylase solution and 500 µl 0.02 M sodium phosphate buffer (pH 6.9) for 10 min at 25 °C in one set of tubes. In another set of tubes α-amylase was pre-incubated with 500 µl 0.02 M phosphate buffer (pH 6.9). Various aliquots starch solution at increasing concentration s of (2–8 mg/mL) was added to both set of tubes to initiate the reaction. The mixture then incubated at 25 °C for 10 min, and then boiled for 5 min then 500 µl of dinitrosalicyclic acid (DNS) reagent was added to stop the reaction. The amount of reducing sugars released was determined by using maltose standard curve and converted to reaction velocities. A double reciprocal plot (1/v vs 1/S) was plotted where S was substrate concentration and v was velocity. Inhibitory effect of nanoemulsions on on α-amylase activity was monitored Lineweaver-bulk by Michaelis–Menten kinetics.

2.11 Antifungal activity

The antifungal activity of nanoemulsions was determined according to technique described by Gakuubi et al., [16]. The antifungal activity of nanoemulsions against *Aspergillum fumigatum* was determined according to zone of inhibition agar disc diffusion method. Briefly, 10 agar discs with mycelia (10 mm in diameter) were taken from periphery of actively growing 7-day old pure culture of *Aspergillum fumigatum* suspended in 15 mL of sterile H_2O. 100 µl of this fungal suspension was used as inoculums and was evenly spread on petri plates containing PDA media. The plates were kept standing at room temperature for 20 min. Sterilized paper discs (15 mm in diameter) impregnated nanoemulsions (200µλ) were placed in centre of each agar plates and incubated at 37 °C for 7 days. Antibiotic disc of 30µg tetracycline was taken as positive control.

2.12 Anti-bacterial activity

The in vitro antimicrobial activity of nanoemulsions was determined through agar disc diffusion method against four test organisms, gram-negative *Escherichia coli* (MTCC 40), *Pseudomonas aeruginosa* (MTCC 424), and Gram-positive *Staphylococcus aureus* (MTCC 3160) and *Bacillus subtilis* (MTCC 121), following Sharma et al. [14, 15]. Pathogens were purchased from Institute of Microbial Technology, Chandigarh. Sterile paper discs (10 mm in diameter) were impregnated with 200 µl nanoemulsions. Twelve hour

cultures were used inoculums and OD of suspensions was adjusted to 0.6. A swab of bacteria suspension was spread on to LB-Agar plates and allowed to dry for 30 min. The discs with nanoemulsions were then applied and plates were left for 20 min at room temperature to allow to diffusion of oil followed by incubation at 37 °C for 24 h. Zone of inhibition was measured.

2.13 Total phenolic content

The total phenolic content of LGO was determined by the method described by Sharma et al. [14]. Gallic acid was taken as standard (calibration curve). Results were expressed as mg Gallic Acid Equivalent (GAE)/ mL using standard equation $y = 0.022x + 0.290$, $R^2 = 0.832$. All samples were analyzed in triplicates.

2.14 Determination of flavonoid content

The total flavonoid content of LGO was determined by the method described by Sharma et al. [14]. Determination was calibrated with standard curve of prepared Rutin solution. Results were expressed as mg Rutin Equivalent (RUE)/ mL using standard equation $y = 0.020x + 0.270$, $R^2 = 0.88$. All samples were analyzed in triplicates.

2.15 Statistical analysis

Each values is mean ± SE ($n = 3$). Tukey HSD test was used to determine P values using SPSS 26.0 (IBM, Armonk, NY, USA). Values of $P < 0.05$ were significant.

3 Results and discussion

3.1 Physiochemical studies

In aromatic plants, essential oils are one among many secondary metabolites which are known to be biological active and to poses potent pharmacological activities. As the essential oils are extracted from plants, being natural are preferred over synthetic ones because of safety concerns [3–5]. In the present study, the total phenolics, and total flavonoids were estimated to be 28.76 mg/g GAE, and 3.4 mg/g RE, respectively (S. Table 2). The content of phenolics was found higher than flavonoids. Due to these phytochemicals, lemongrass oil has a wide range of applications, as effective antifungal and antibacterial agents and being used in perfumery, scenting soaps, hair oils, cosmetics and as an insect repellent [2–5].

Essential oil derived from *Cymbopogon pendulus*, lemon grass, is highly unstable, volatile and prone to oxidation under normal conditions, hence in order to improve its Pharmokinetic profile, it must be incorporated into O/W type of nano-emulsions. So in this study, six different nanoemulsions designated as F1 to F6 were developed and main physiochemical parameters examined. Physiochemical and morphological of formulated nanoemulsions are depicted in Fig. 1 and Table 1. Morphological studies revealed that all formulated nanoemulsions were circular, smooth and non-aggregated. Formulated nano-formulations were kinetically stable as there was no gravitational separation [9]. The mean diameter of F1 and F2 nanoemulsions synthesized by using tween 20 was 463 and 511 nm. SDS decreased particle size significantly. F3 and F4 nanoemulsions were smaller (mean diameter 340 and 400 nm, respectively). Notably, it was observed that co-surfactant ethanol substantially decreased mean diameter of F5 and F6 ethanol containing nanoemulsions was 327 nm and 397 nm, respectively. These observations were in consonance with Silva et al., [17] and Qian and McClements [12], indicating that several factors like adsorption rate, thickness, charge, permeability could be the reasons. All O/W nanoemulsions did not show any sign of phase inversion in dye solubility test thus established the formulated nanoemulsions were stable.

pH and conductivity of nanoemulsions were monitored (Table 1). Conductivity depicts electrical conductivity [18]. F1 (prepared with Tween 20) and F2 (prepared with Tween 80) displayed conductivity values 0.06 and 0.09, respectively**.** Notably, in F1 and F2 nanoemulsions, when surfactant SDS was added, a sharp increase in conductivity was observed (F3 and F4). This observation may be plausible to increase in number of free ions which drastically increased conductivity of nano-formulations. Turbidity studies that determine qualitative and quantitative changes at 600 nm using UV–VIS spectrophotometer illustrated that turbidity of ethanol based F5 and F6 nanoemulsions was higher than all other formulations (Fig. 1) Kumar et al., [19] and Tomaszewsk et al. [20] documented that nanoemulsions optical properties is highly influenced by number of factors including size, shape and concentration.

3.2 Fingerprint analysis

Secondary metabolites fingerprint characterization by spectroscopy techniques like ultraviolet, fluorescent and FT-IR spectroscopy provides valuable insights about qualitative and quantitative formulation of herbal derivatives for detecting phytocomponents [20]. UV-profile of all nano-formulations (F1 to F6) revealed sharp peaks at about 250 nm (Fig. 2A), is indicating the occurrence of bioactive molecules. Presence of citral in these LGO nano-emulsions were also confirmed by their UV–VIS spectrum as citral peak in range of 320–360 nm is observed in all formulations. Notably, when LG oil was encapsulated, both F5 and F6 nanoemulsions depicted increased absorbance which may be ascribed to less

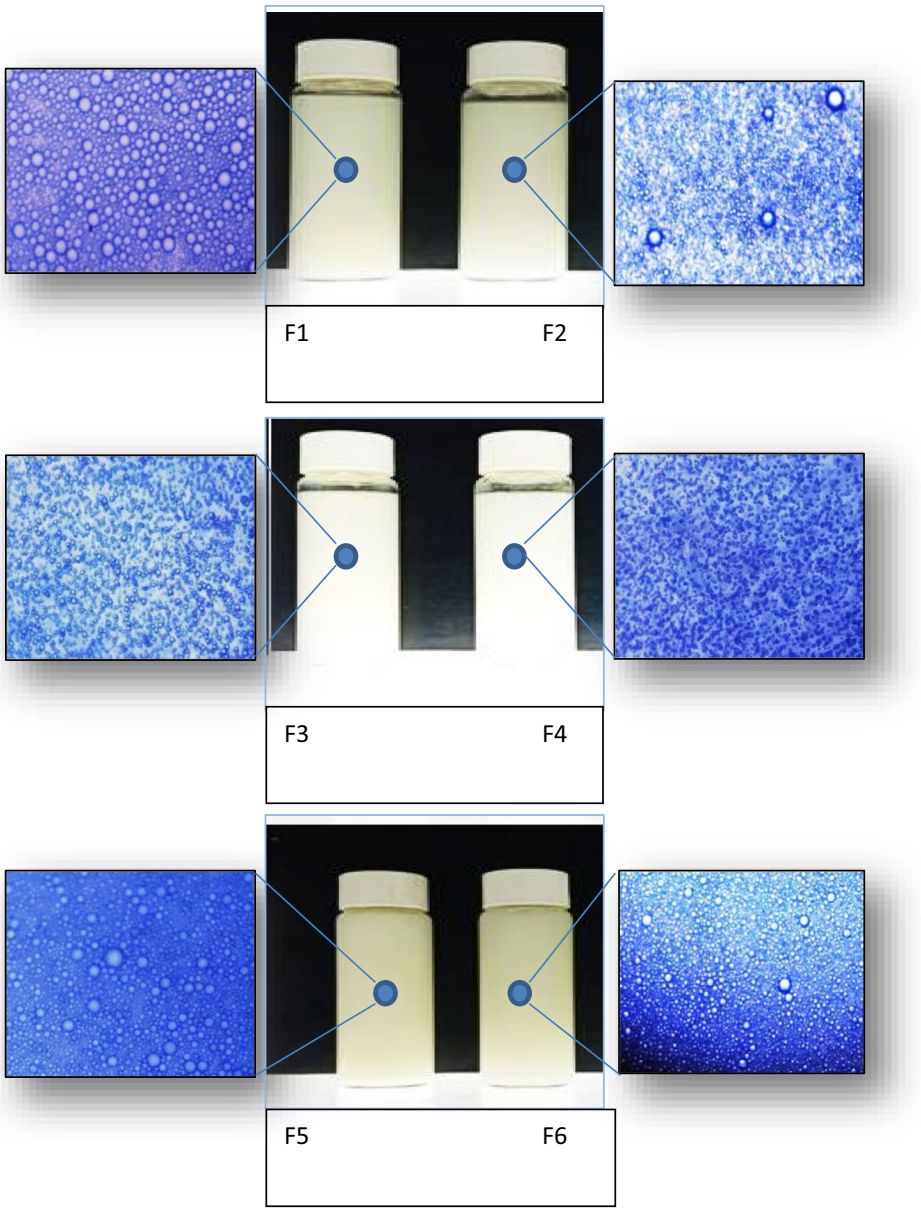

Fig. 1 Morphological view of nanoemulsions

Table 1 Physiochemical parameters of nanoemulsions (mean ± S.D, $n = 3$)

Parameters	Formulations					
	F1	F2	F3	F4	F5	F6
STRUCTURE TYPE	O/W	O/W	O/W	O/W	O/W	O/W
MEAN SIZE (nm)	463 ± 5^{a}	511 ± 10^{b}	340 ± 10^{c}	400 ± 11^{d}	327 ± 5^{e}	395 ± 10^{f}
OD AT 600 nm	0.200 ± 0.2^{a}	0.315 ± 0.04^{b}	0.526 ± 0.02^{c}	0.424 ± 0.04^{d}	0.642 ± 0.04^{e}	0.692 ± 0.01^{e}
PH	8.14 ± 1^{a}	8.37 ± 1^{a}	8.42 ± 2^{a}	8.70 ± 2^{b}	8.93 ± 2^{b}	8.84 ± 1^{b}
CONDUCTIVITY	0.076 ± 0.3^{a}	0.093 ± 0.02^{a}	0.209 ± 0.03^{b}	0.268 ± 0.03^{b}	0.028 ± 0.04^{c}	0.042 ± 0.02^{d}

[a,b,c,d,e]Different letters with in row indicate significant difference at $P \leq 0.05$

particle size of nanoemulsions with huge surface area. Under florescent emission studies, as demonstrated in Fig. 2B, pure oil displayed one sharp peak at 500 nm (green fluorescent region). Flavonoids, flavins and terpenoids are the bioactives responsible for green fluorescent region emission (lambda near 500 nm) [21]. Notably, when oil was entrapped in

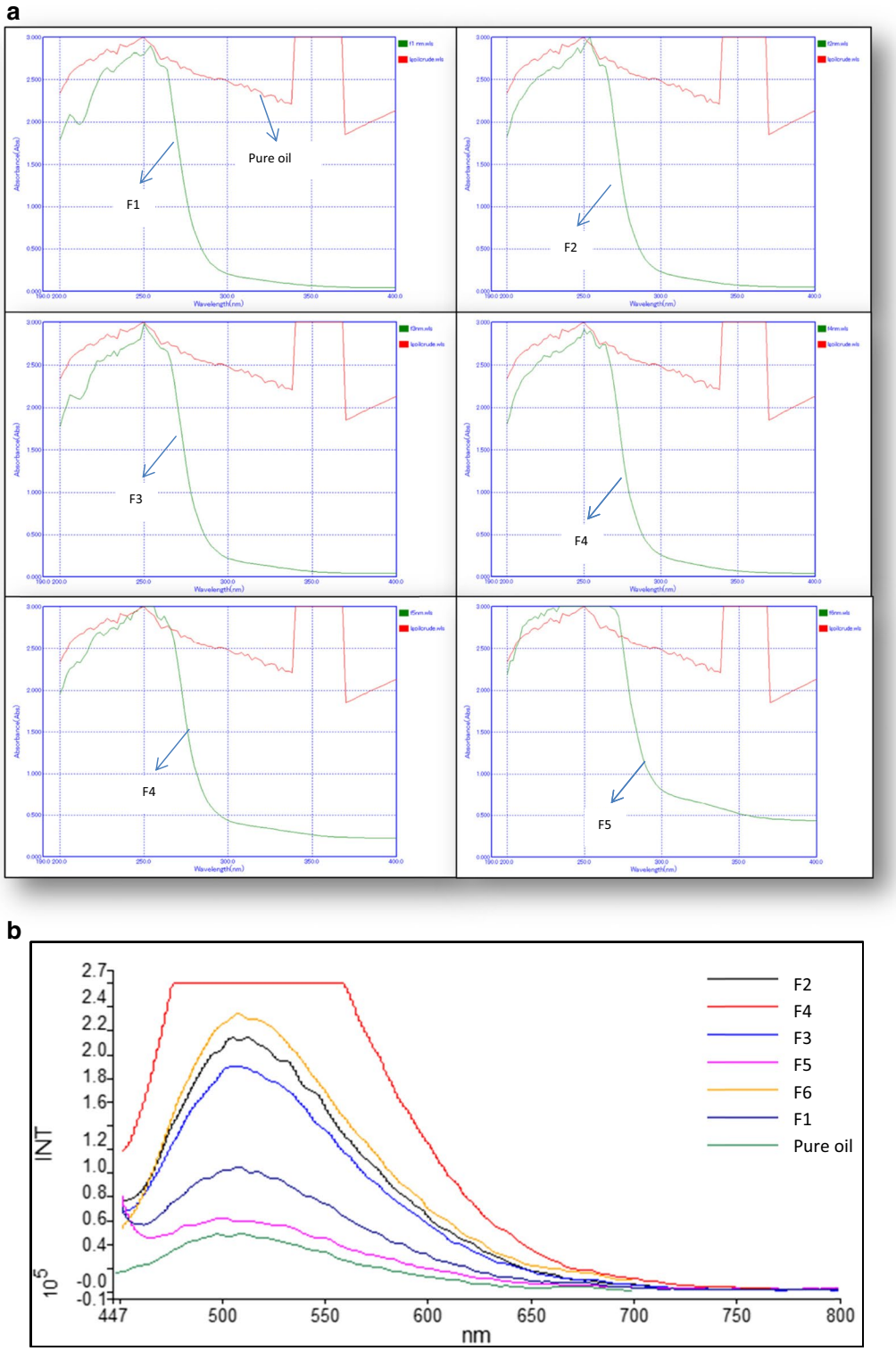

Fig. 2 A UV-Profile of Nanoemulsions, F1–F5 indicates different nanoemulsions. B Fluorescent spectral analysis (B)

form of nano-formulations a strident increase in fluorescent intensity was practical. Boni et al., [22] also cited that micro emulsion exhibited enhanced fluorescent signals. Authors claimed that nano-droplets enhanced the scattering of light by acting as optical signal amplifier.

Functional group analysis of bioactives present in LGO was studied by Fourier Transform Infrared

Spectrophotometer (FT-IR) which is posed to be powerful, rapid, non-destructive method for fingerprint analysis plant extracts [20]. It is a powerful tool for identifying diverse types of chemical bonds in a molecule by producing an infrared absorption spectrum. Vibrational energy levels of oscillations of atoms in secondary metabolites molecules were measured by FT-IR Spectrometer. It provides energy levels that are directly proportional to molecular structure, intermolecular interaction, and the chemical bonding. FT-IR peak values for LGO are given in Fig. 3. LGO revealed the presence of different functional groups in bioactive compounds. In FT-IR spectrum broad peak at 2923 cm^{-1}

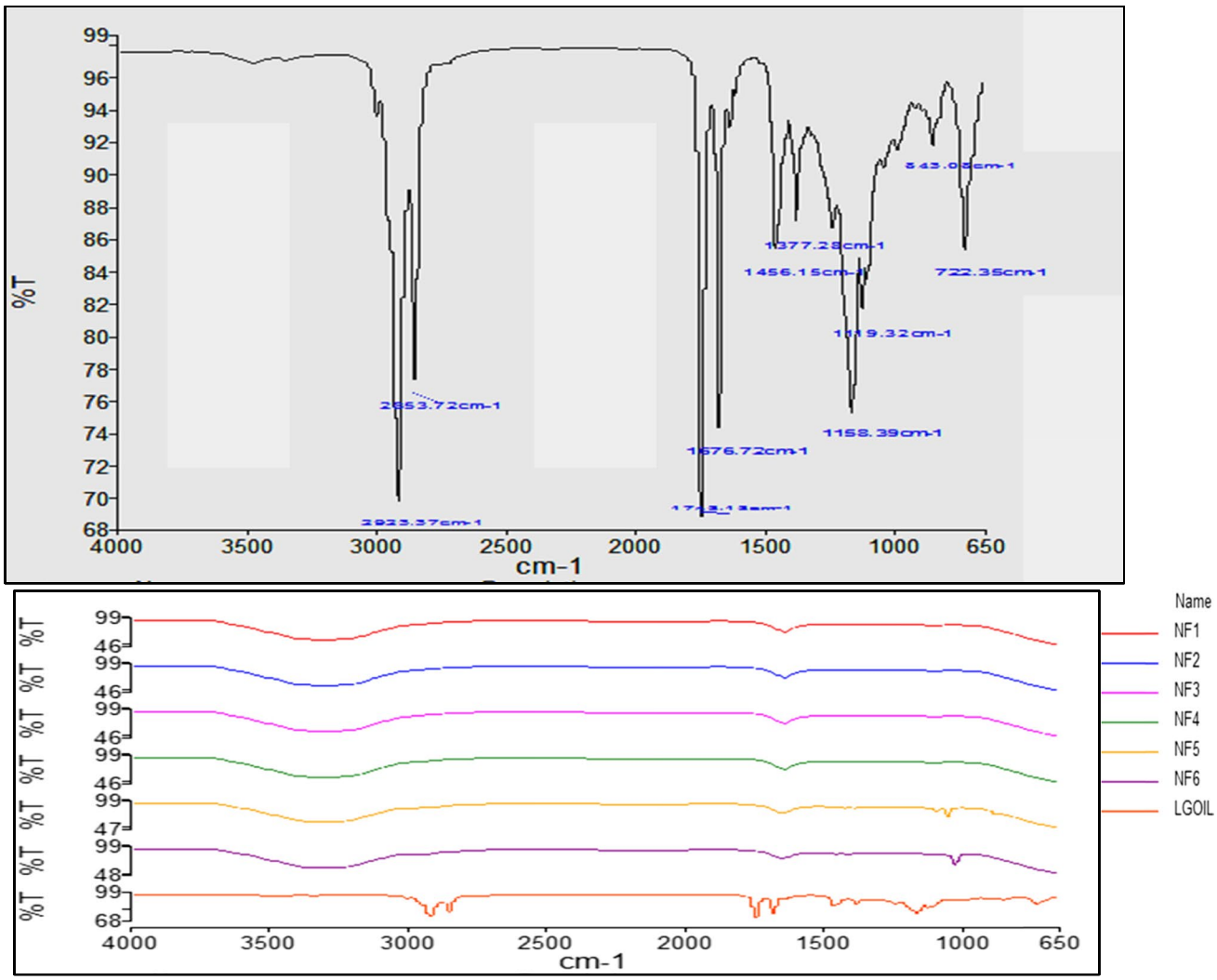

X (cm^{-1})	Y (%T)	VIBRATION MODE	FUNCTIONAL GROUP
2923.37	70	C-H stretching	Alkene
2853.72	77	C-H stretching	Alkane
1713.12	69	C=O stretching	Acid Halide
1676.72	74	C=N stretching	Amines
1456.15	86	C-H bending	Alkane
1377.28	88	S=O stretching	Sulphonamide Sulphonate
1158.39	76	C-O stretching	Tertiary Alcohol
1119.32	82	C-O stretching	Aliphatic Ether 2°-Alcohol
843.03	92	C=C bending	Alkenes
722.35	86	C-H bending	Trisubstituted alkenes

Fig. 3 FT-IR profile and peak values of lemongrass essential oil

indicated C-H stretching due to alkenes, peak at 1456 cm^{-1} attributed to C-H bending due to alkanes and peak at 1377 cm^{-1} shows S = O bending due to sulphonamides, peaks around 1158 cm^{-1} and 1119 cm^{-1} were due to aliphatic ether and alcohols respectively. Pure LG oil depicted two major IR bands at about 1734 cm^{-1} and 1672 cm^{-1} due to C = O stretching of acid halides and C = N stretching of amines, respectively. Because each of the secondary structure was associated with a characteristic hydrogen bonding pattern hence, it was expected that each type of secondary structure will give rise to characteristic absorptions by IR spectroscopy. Similar bioactive peaks of aromatic compounds, alcohols, phenols, alkanes, alkynes, and amines in LGO have been reported *Cymbopogon citratus* [23]. All these bioactives are classified as plant secondary metabolites [24], which could be the possible reason behind various bioactivities and medicinal properties of LGO.

Encapsulation of oil with in nanoemulsions was further evaluated by FT-IR spectroscopy. FT-IR spectroscopy was used to find out interactions about the complex formation and interaction of major functional groups involved in the encapsulation of essential oil [20]. FT-IR results helped us in confirming the presence of LGO in prepared nanocapsules. In comparison with pure LG oil, nano-formulations exhibited a different FT-IR spectrum. The peak at 1672 cm^{-1} was almost there in F1–F6 formulations, but there was a slight shift to lower wavelength. It was also evident that there were some minor and major peaks, which were formed when LG essential oil was encapsulated as shown Fig. 3. For instance: in all nano-formulations, one prominent band at 3400 cm^{-1} and 1000 cm-1, was observed which were absent in pure LG oil. These kind of shifts and new IR bands in FT-IR profile implied that LG oil effectively encapsulated in the micelle structure of mixed surfactant during preparation of LG nanoemulsions droplets. FT-IR spectroscopy is widely used for studying the interactions between drug and excipients. Kumar et al. [25] also documented similar findings in eucalyptus essential oil upon encapsulation. Yan et al. (9) also reported similar observations during encapsulation of bifenthrin in biodiesel based O/W nanoemulsions. Due to these bioactives lemon grass oil is immensely used in various aspects of medical sciences [2–4].

3.3 Storage stability

To use as anti-microbial agents in drug delivery system, long-term stability with time is the major factor in synthesis of nanoemulsions. F1 to F6 nano-emulsions were used to study stability studies under different environmental stress-like conditions. The nanoemulsions were further selected for centrifugation analysis. Notably, no signal of cracking or creaming or phase inversion was detected. Formulated nanoemulsions were kinetically stable as there was no gravitational separation. No change in pH of all nano-formulations was observed (data not shown), indicating that encapsulation prevented degradation of bioactives upon storage. To analyze shelf-life and long-term steadiness of nanoemulsions, augmented stability studies were conducted at 3 diverse temperatures for 50 days. As observed in results, F1 nanoemulsions no change in particle size was observed at 4 °C and -20 °C, however, nano-emulsion cracking was detected at 37 °C (Fig. 4). In other F2. F4, F5 nanoemulsions, there was no sign of change in particle size at 4 °C and -20 °C, while, at 37 °C ostwald repining was detected. Ostwald repining is a process in which small nano-droplets merged to bigger one due to diffusion of oil through intervening aqueous phase [25, 26]. Therefore, cold temperature was required to prevent, Ostwald ripening, coalescence and flocculation. From above observations, it was perceived that synthesized nanoemulsions were stable over 50 days at 4 °C and could be best candidates for industrial applications.

3.4 Anti-inflammatory activity

It was well established that the major reason behind tissue inflammation is protein denaturation. It is accompanied by loss of tertiary and secondary protein structures which is associated with red- ness, swelling, heat or loss of function at infected tissues [19]. Therefore, bioactive molecules that prevent protein denaturation are supposed to be the best therapeutic candidates as anti-inflammatory agents. This study reports protein denaturation inhibitory ability of nanoemulsions by adopting tryptophan fluorescence spectroscopy technique [14, 15]. As illustrated in Fig. 5, all nanoemulsions when added to BSA, marked decrease fluorescence intensity was observed. However, inhibition of protein denaturation was observed in a type of nanoemulsions dependent manner. For example, maximum inhibition in protein denaturation was observed with F6 nanoemulsions, as the magnitude of decrease was more in F6 than other Nano-formulations (Fig. 5B). These findings highlighted that lemon grass oil based nanoemulsions poses potential to act as anti-inflammatory agents in corroboration with earlier findings on plant based bioactive molecules as anti-inflammatory agents [19].

3.5 Antibacterial properties of nanoemulsions

The antibacterial activity of nanoemulsions was measured against drug resistant microbial strains of *Escherichia coli* (MTCC-40), *Bacillus subtilis* (MTCC-121), *Pseudomonas aeruginosa* (MTCC-424), and *Staphylococcus aureus* (MTCC-3160), the results of which are depicted in Table 2. The present study shows that F1 and F2 nanoemulsion formulations exhibits total inhibition against gram-negative *Escherichia coli* (MTCC-40), gram-positive *Bacillus subtilis* (MTCC-121), and *Pseudomonas*

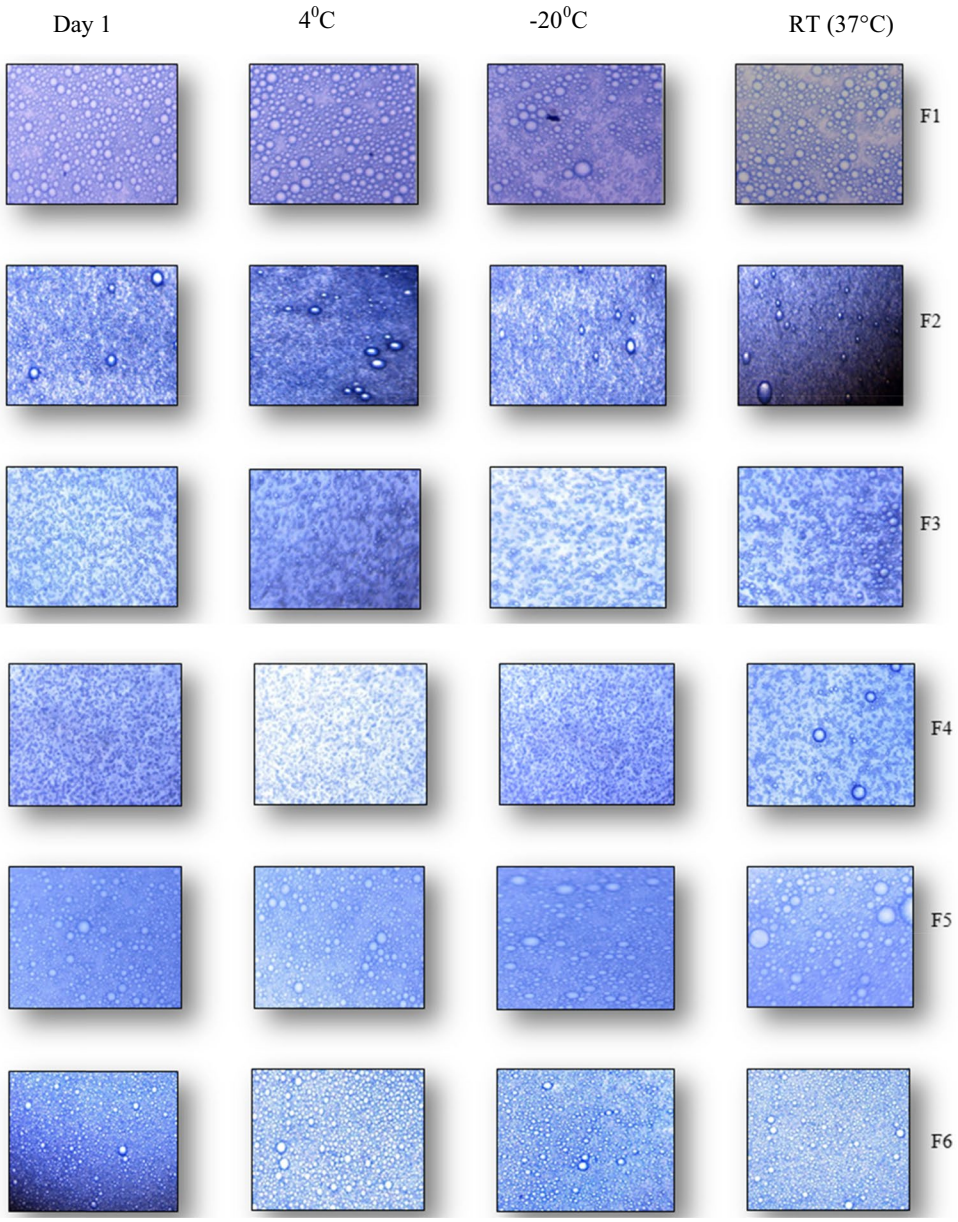

Fig. 4 Storage stability of nanoemulsions after 50 days at different temperatures

aeruginosa (MTCC-424) and moderate antimicrobial activity against *Staphylococcus aureus* (MTCC-3160). F3 nano-emulsion formulation exhibits total inhibition against *Staphylococcus aureus* (MTCC-3160), high antimicrobial activity against *Bacillus subtilis* (MTCC-121) while moderate activity against *Escherichia coli* (MTCC-40) and *Pseudomonas aeruginosa* (MTCC-424). F4 nano-emulsion formulation exhibits total inhibition against *Bacillus subtilis* (MTCC-121) and *Pseudomonas aeruginosa* (MTCC-424) while moderate activity against *Escherichia coli*, MTCC-40 and *Staphylococcus aureus* (MTCC-3160). F5 nano-emulsion formulation depicted high antimicrobial activity against *Bacillus subtilis* (MTCC-121), moderate activity against *Staphylococcus aureus* (MTCC-3160) and *Escherichia coli* (MTCC-40) and total inhibition against *Pseudomonas aeruginosa* (MTCC-424). F6 nano-emulsion formulation exhibits similar antimicrobial activity like F4 nano-emulsion formulation. The high antimicrobial activity of nano-emulsion formulations might occur due to their interaction with microbial cell membrane as a result of large surface area and passive transport across cell membrane, fusion of nano-particle (emulsion) with cell membrane, stability of essential oil constituents and their sustained release or by electrostatic interaction between nano-emulsion and microbial cell wall, which lead to increase in concentration of essential oil or its constituent at target site [6, 27]. The present study also revealed high antimicrobial toxicity of LGO nano-emulsions toward gram negative bacteria which is a noteworthy observation as most literature suggests that the gram negative bacteria

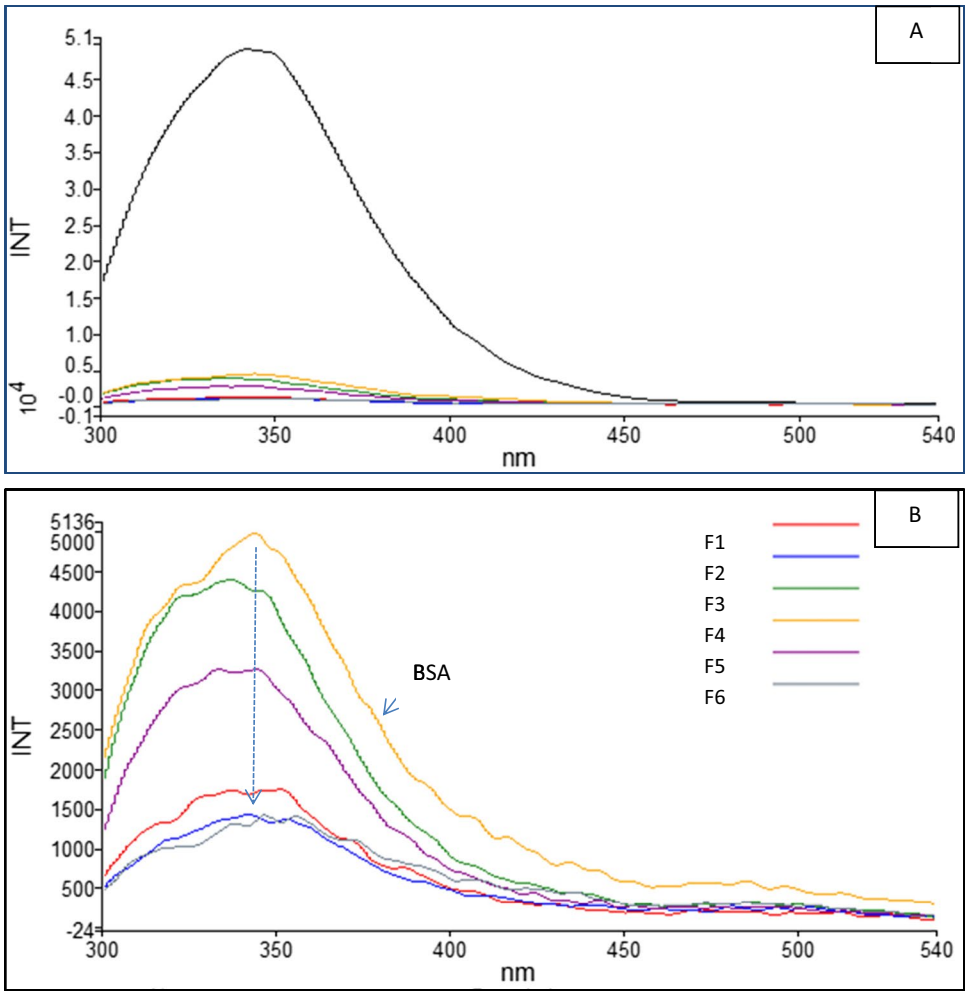

Fig. 5 Protein denaturation (tryptophan fluorescent spectroscopy) analysis of nanoemulsions

are more resistant than gram positive bacteria due to complex nature of cell wall [27]. Presence of phospholipids, lipopolysaccharides (LPS), and thick peptidoglycan layer allow gram-negative bacteria to be more resistant to most of the hydrophobic antibiotics and toxic drugs.

3.6 Anti-fungal activity

The antifungal activity of LG oil-based nanoemulsions was checked against *Aspergillum fumigatum* which is responsible for causing "aspergillosis" in immune-competent COVID-19 patients [28]. Aspergillosis is a type of infection which is

Table 2 Anti-bacterial activity of LGO nano-emulsion formulations

S.NO	Sample control	Sample volume (uL)	ZOI (cm) MTCC -40	ZOI (cm) MTCC -121	ZOI (cm) MTCC -424	ZOI (cm) MTCC -3160
1	NC	0	NI	NI	NI	NI
2	PC	30 mcg				
3	F1	200	TI	TI	TI	3.5^a
4	F2	200	TI	TI	TI	2.8^b
5	F3	200	3.4^a	5.0^a	3.2	TI
6	F4	200	2.8^b	TI	TI	4.0^c
7	F5	200	3.2^c	5.6^a	TI	3.8^c
8	F6	200	3.2^c	TI	TI	4.2^c

Different letters with in column indicate significant difference at $P \leq 0.05$ with in column

caused by invasive common mold "Aspergillus", that exists outdoors and indoors. The rapid rise in fungal infections post 2nd wave of COVID-19 was attributed to the un-regulated use of steroids for COVID patients. It was observed that this fungus is affecting immune-compromised individuals like COVID-19 patients on recovering state and have diabetes or high un-controlled sugar levels. [29]. The symptoms of invasive aspergillosis are running nose, headache, stiffness, chest pain, cough, blood in cough, fever, reduced ability to smell, and breathing problems. In this study, the antifungal activity of LGO is given in Table 3 (supplementary Fig. 1), respectively. F1 to F4 nanoemulsions affected fungal growth effectively. However, very high antifungal activity of F5 and F6 nanoemulsions was observed as total inhibition in fungal growth was observed. These results were supported by the work of Boukhatem et al., [4] citing inhibitor role of lemon grass oil against athlete's foot, ringworm, jock itch, and yeast infections. The possible reason behind high antifungal activity of LGO was its high citral and polyphenolic content. Citral, a monoterpene, occurs naturally in herbs, plants, and citrus fruits and possesses high antifungal, insecticidal, and bactericidal activity [27]. In general, essential oils as a potent natural antifungal compounds have been reported earlier D'agostino et al., [30]. The possible anti-fungal mechanism is that due to lipophilicity nature of LGO, it easily penetrates fungus cell wall that finally inhibits fungal hyphal-growth or a decrease in the production and germination of conidia of fungal strains. Gao et al. [31] also reported that at a high concentration of oils, the fungal hyphae collapse and break down which finally damages the cytoplasmic membrane, leading to the leakage of electrolytes and possibly lipid peroxidation due to ROS generation induced by the increase in permeability. Singh et al. [32] also demonstrated that due to the presence of bioactive like geraniol, that is found abundantly in lemongrass and aromatic herbs, essential oils may induce an inhibitory effect on the calcineurin pathway which leads to a decrease in the plasma membrane permeability and damage of the cell wall.

Table 3 Anti-fungal activity of LGO nano-emulsion formulations against *Aspergillum fumigatum*

S.NO	Sample/control	Sample volume (uL)	Day 7 (ZOI)
1	NC	0	NI
2	PC (30 ug)	30ug	NI
3	B1	200	NI
4	F1	300	4.5^{a}
5	F2	300	2.5^{b}
6	F3	300	3.4^{a}
7	F4	300	3.5^{a}
8	F5	300	TI
9	F6	300	TI

Different letters with in column indicate significant difference at $P \leq 0.05$ with in column

Table 4 Drug entrapment efficiency of nano-emulsions

Nanoemulsion formulation	Entrapment (%)
F1	41.50 ± 5a
F2	49.88 ± 4b
F3	51.41 ± 3b
F4	55.34 ± 2b
F5	60.13 ± 2c
F6	60.23 ± 2c

Different letters indicate with in column significant difference at $P \leq 0.05$ with in column

Encapsulation efficiency, drug release study, and kinetics.

Encapsulation efficiency (EE) of nanoemulsions is indicated in Table 4. It was observed that EE enhanced substantially upon reducing the size of droplets. It was observed that upon adding SDS and ethanol, droplet size decreased coupled with increased in EE. For instance: EE of F1 increased from 41 to 51%, F2 increased from 49 to 55%. Drug entrapment efficiency of F5 and F6 was higher (60%) as compared to other formulations. Earlier studies have indicated that emulsion droplet size has a key effect on the EE of different core materials [33]. Reducing the emulsion droplet size can result in higher retention of encapsulated components in emulsion systems. The greater retention of oil in small emulsion droplets is related to the reduced mean diameter of volume surface, which can enhance the modification of spherical interface organization and increase the interfacial area to govern the partition of aroma compounds in emulsions [34]. Due to having high EE, F5 and F6 formulation were used for further drug release and pharmokinetics studies. In-vitro drug release of pure oil and nanoemulsions was studied. As shown in Fig. 6, it was found that owing to lipophilic and

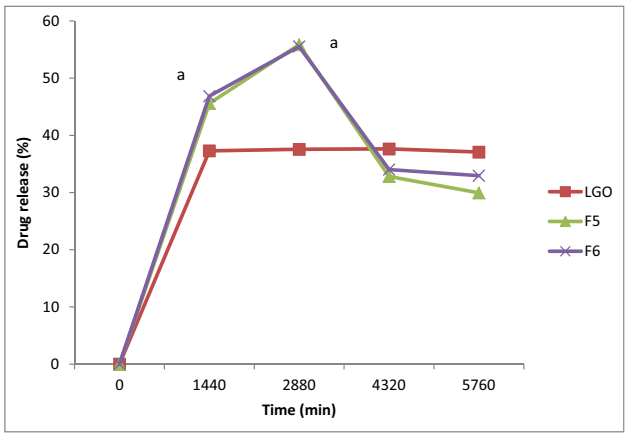

Fig. 6 In vitro drug release profile of F5 and F6 nanoemulsions: a:indicates significant difference vs LGO at $P \leq 0.05$ with in column

low water solubility, pure oil showed in vitro drug release of 37%, while F5 and F6 formulations led to increase in dissolution rate with 66% drug release while F2 was 45% and 46% in 24 h which further raised to almost 55%. This could be attributed due to small droplet size and eventually large surface area of small droplets of emulsions, that provided nanoemulsions better release profile than plan pure oil.

To get insight into the mechanism of drug release, four kinetic models like zero order (% drug release vs. time), first order (log % drug remaining vs time); Korsmeyer–Peppas model (log % drug release vs log time); Higuchi model (% drug release vs square root of time) were evaluated. Release of essential oil from nano-formulations was monitored with these models. High correlation coefficient (R^2) value was evaluated that indicates best fit model to depict release

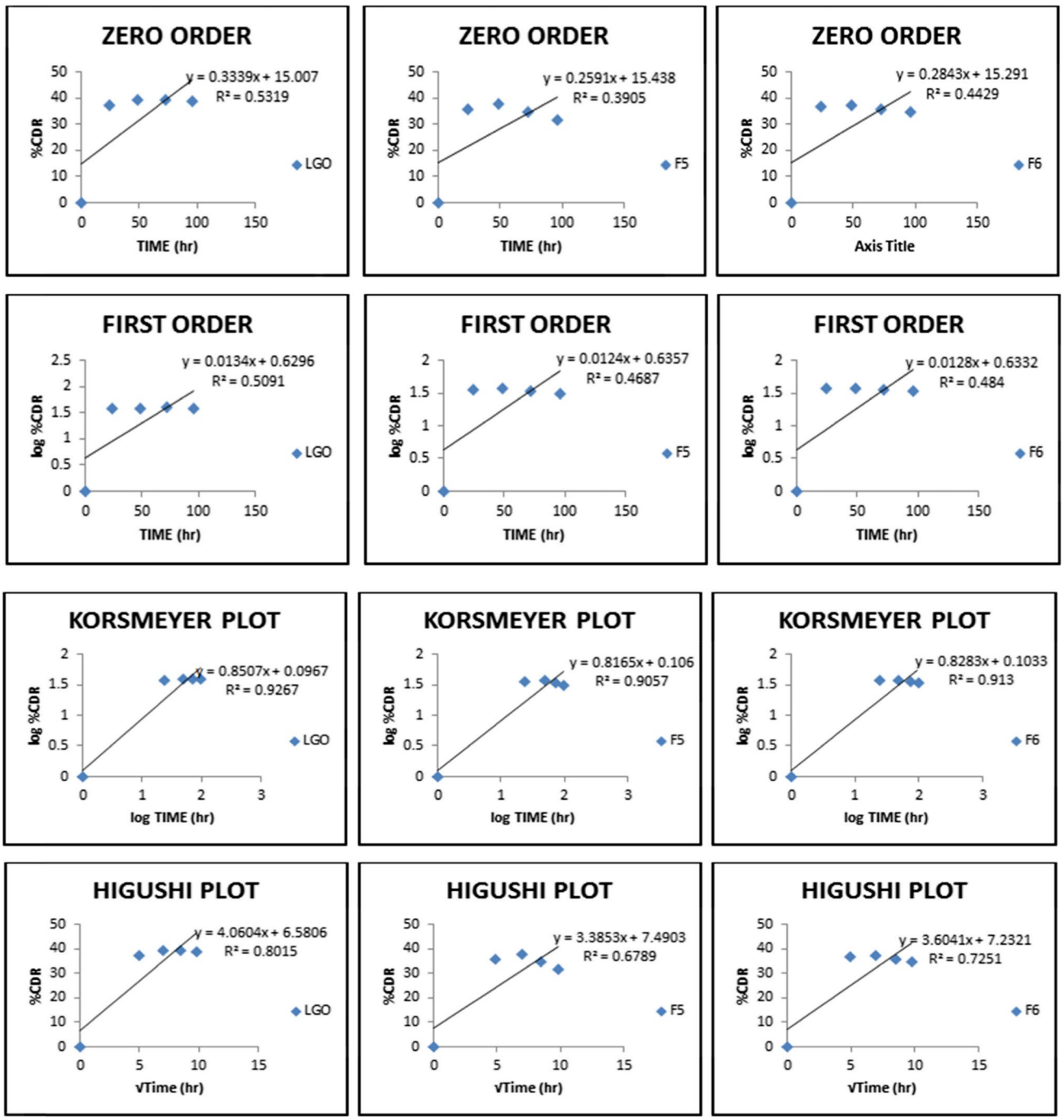

Fig. 7 Drug kinetics of F5 and F6 nanoemulsions

pattern of essential oil (Fig. 7). It was observed that F5 and F6 nanoemulsions follow the Korsmeyer-Peppas model as *R* value for this model was 0.90 (F5) and 0.91 (F6). The release diffusion exponent values were $n = 0.81$ (F5) and 0.82 (F6), that designates release mechanism is Fickian diffusion. Our findings were in corroboration with findings of Laxmi et al. [35] citing artemether nanaoemulsions.

3.7 Anti-diabetic (alpha-amylase inhibition) activity

The inhibition of alpha-amylase activity by various inhibitors mainly aimed to delay the carbohydrate metabolism thus controls blood glucose level diabetic patients [36]. Many strategies involve inhibition of key enzymes of carbohydrate metabolism like alpha amylase to cure diabetes mellitus. To find out potency of LGO based F5 and F6 nanoemulsions to be used as an alternate anti-diabetic drug with less toxicity and more potency than existing drugs. In this study, various fractions of F5 and F6 LGO nanoemulsions were used to determine is anti-diabetic capability. Both LGO nano-emulsion formulations showed high inhibition of alpha-amylase activity in a dose dependent manner as depicted in Fig. 8. F6 nano-emulsion formulation showed slightly less inhibition as compared to F5 nano-emulsion formulation. The present study suggests that inhibitory activity of these nano-emulsion formulations may arise due to high anti-diabetic activity of LGO [3]. The mode of inhibition of F5 and F6 LGO nano-emulsion formulations was determined using Michaelis–Menten plot and Lineweaver–Burk plot as depicted in Fig. 8 and which displays near competitive inhibition. The present study suggests that LGO nanoemulsions exhibit its hypoglycemic potential. The results obtained were supported by findings of Oladeji et al., [3]. Previous studies of inhibitory action of various plant-based inhibitors indicated that these inhibitors majorly belong to flavonoids that contain the features of inhibiting alpha amylase activity [35–37].

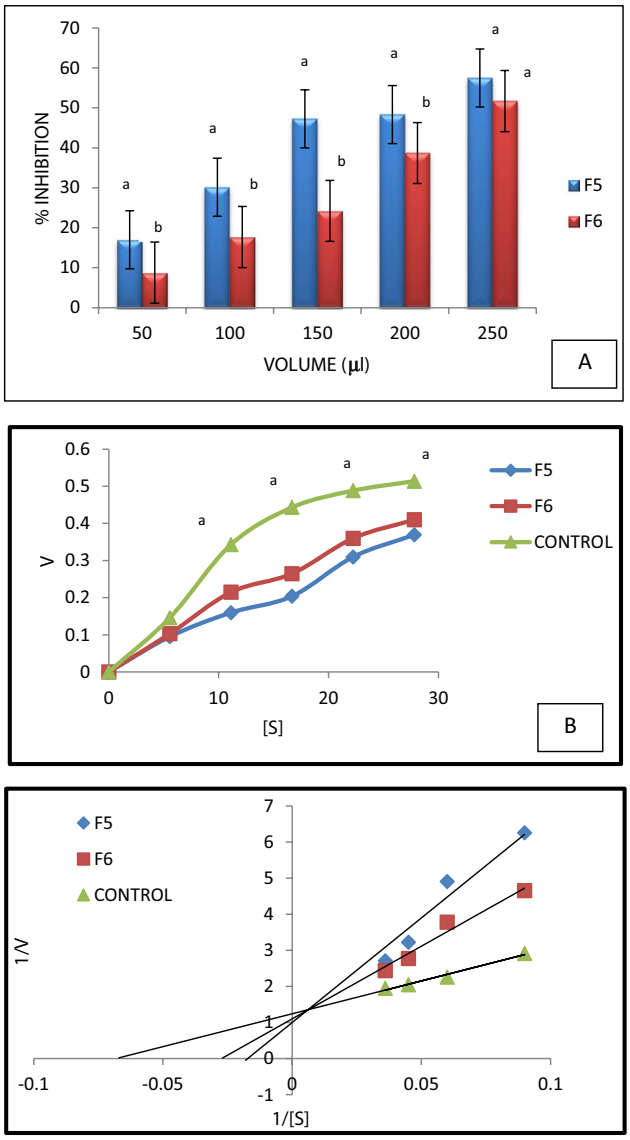

Fig. 8 Anti-diabetic assay for LGO nano-emulsions (F 5 and F6), Lineweaver–Burk and Michaelis–Menten plot for F5 and F6 LGO nano-emulsions. Different letters in "A" panel indicates significant difference among F5 and F6 at $P \leq 0.05$. Different letters in "B" panel indicates significant difference of F5 and F6 vs control at $P \leq 0.05$

4 Conclusion

Formulated nanoemulsions were evaluated in terms of pH, conductivity, and size. All nanoemulsions were in morphologically good and circular. The mean diameter of F1 and F2 nanoemulsions synthesized by using tween 20 was 463 and 511 nm. But SDS decreased particle size significantly (F3 and F4 nanoemulsions). Remarkably, it was observed that co-surfactant ethanol substantially decreased mean particle size. Notably, when surfactant SDS was added, a sharp increase in conductivity was observed. Turbidity of ethanol based F5 and F6 nanoemulsions was higher than all other formulations. Even after 50 days of storage, nanoemulsions were stable as no phase separation, cracking and flocculation was observed. Further, nano-formulations exhibited good anti-inflammatory, anti-bacterial, and anti-diabetic activities. Based on these findings, it was postulated that lemon grass oil-based nano-emulsions may be a cost-effective technique with apposite prospective in a range of applications in the area of cosmetic, food, and pharma-based cosmetic industries in future.

Supplementary Information The online version contains supplementary material available at https://doi.org/10.1007/s12668-022-00964-4.

Acknowledgements DST, SEED and FIST lab LKC.

Funding Project is funded by DST, SEED.

Declarations

Research involving humans and animals statement None.

Informed consent The authors gave consent for MS.

Conflict of interest None.

References

1. Raho, G. B., & Benali, M. (2012). Antibacterial activity of the essential oils from the leaves of *Eucalyptus globulus* against Escherichia coli and *Staphylococcus aureus*. *Asian Pacific Journal of Tropical Biomedicine, 2*, 739–742.
2. Goodger, J.Q.D., Senaratne, S.L., Nicolle, D., Woodrow, I.E., (2016). Correction: Foliar Essential Oil Glands of *Eucalyptus* Subgenus *Eucalyptus* (Myrtaceae) Are a Rich Source of Flavonoids and Related Non-Volatile Constituents. PLOS ONE. 11: e0155568
3. Oladeji OS, Adelowo FE, Ayodele DT, Odelade KA. 2019. Phytochemistry and pharmacological activities of *Cymbopogon citratus*: A review. Scientific African, 6, e00137
4. Sharma S, Shagufta Habib, Debasis Sahu, Jeena Gupta. Chemical properties and therapeutic potential of citral, a monoterpene isolated from lemongrass. Medicinal Chemistry 17 (1), 2–12, 2021.
5. Boukhatem, M. N., Ferhat, M. A., Kameli, A., Saidi, F., & Kebir, H. T. (2014). Lemon grass (Cymbopogon citratus) essential oil as a potent anti-inflammatory and antifungal drugs. *Libyan Journal of Medicine, 9*, 25431.
6. Moghimi, R., Ghaderi, L., Rafati, H., Aliahmadi, A., & McClements, D. J. (2016). Superior antibacterial activity of nanoemulsion of Thymus daenensis essential oil against E. coli. *Food Chemistry, 194*, 410–415.
7. Ines, G. R. M., Juliana, M. C., Araceli, O. M., Laura, S. T., & Olga, M. B. (2015). Long-term stability of food-grade nanoemulsions from high methoxyl pectin containing essential oils. *Food Hydrocollogy, 52*, 438–446.
8. Donsi, F. (2018). "Applications of nanoemulsions in foods," in *Nanoemulsions: Formulation, Applications, and Characterization*, eds S. M. Jafari and D. J. McClements (Cambridge, MA: Academic Press), 349–377
9. Yan, H., Bao, C. C., Yu, C., Kong, D., Shi, J., & Lin, Q. (2019). Preparation of biodiesel oil-in-water nanoemulsions by mixed surfactants for bifenthrin formulation. *RSC Advances, 9*, 11649–11658.
10. Guglielmini, G. (2008). Nanostructured novel carrier for topical application. *Clinics in Dermatology, 26*, 341–346.
11. Al-Edresi, S., & Baie, S. (2009). Formulation and stability of whitening VCO-in-water nano-cream. *International Journal of Pharmaceutics., 373*, 174–178.
12. Qian, C., Decker, E. A., Xiao, H., & McClements, D. J. (2012). Nanoemulsion delivery systems: Influence of carrier oil on β-carotene bioaccessibility. *Food Chemistry., 135*, 1440–1447.
13. Kerwin, B. A. (2008). Polysorbates 20 and 80 used in the formulation of protein bio therapeutics: Structure and degradation pathways. *Journal of Pharmaceutical Sciences, 97*, 2924–2935.
14. Sharma, A. D., Farmaha, M., Kaur, I., & Singh, N. (2021). Phytochemical analysis using GC-FID, FPLC fingerprinting, antioxidant, antimicrobial, anti- inflammatory activities analysis of traditionally used *Eucalyptus globulus* essential oil. *Drug Analytical Research, 5*, 26–38.
15. Sharma, A., Kaur, I., & Singh, N. (2021). Synthesis, Characterization, and In Vitro Drug Release and In Vitro Antibacterial Activity of O/W Nanoemulsions Loaded with Natural Eucalyptus Globulus Essential Oil. *International Journal of Nanoscience and Nanotechnology, 17*, 191–207.
16. Gakuubi MM, Angeline W. Maina, John M. Wagacha, "Antifungal Activity of Essential Oil of *Eucalyptus camaldulensis* Dehnh. against Selected *Fusarium* spp.", *International Journal of Microbiology*, vol. 2017, Article ID 8761610, 7 pages, 2017
17. Silva, H. D., Cerqueira, M. A., & Vicente, A. A. (2015). Influence of surfactant and processing conditions in the stability of oil-in-water nanoemulsions. *Journal of Food Engineering, 167*, 89–98.
18. Talegaonkar, S., Tariq, M., & Alabood, R. M. (2015). Design and Developement of O/W Nanoemulsion for the Transdermal Delivery of Ondansetron. *Bulletin of Pharmaceutical Research, 1*, 18–30.
19. Kumar, V., Singh, S., et al. (2018). Determination of phytochemical, antioxidant, antimicrobial, and protein binding qualities of hydroethanolic extract of Celastrus paniculatus. *Journal of Applied Biology & Biotechnology, 6*(06), 11–17.
20. Tomaszewsk E, Soliwod K, Kadziol K, Tkacz-Szczesn B, Celichowski G, Cichomski M., Szmaj W, Grobelny J. (2013). Detection Limits of DLS and UV-Vis Spectroscopy in Characterization of Polydisperse Nanoparticles Colloids. Nanomaterials. 1–10
21. Mylle, E., Codreanu, M. C., Boruc, J., & Russinova, E. (2013). Emission spectra profiling of fluorescent proteins in living plant cells. *Plant Methods, 9*, 1–8.
22. Boni, M., Nastasa, V., Andrei, I. R., Staicu, A., Pascu, M. L., "Enhanced fluorescence emitted by microdroplets containing organic dye emulsions", *Biomicrofluidics* , 24 (2015) 9(1) 014126
23. Okpo, S., & Otaraku, I. J. (2020). GC-FID and FT-IR Characterization of Lemongrass Oil Extracted With SOXHLET Extraction Apparatus Using Ethanol as Solvent. *IOSR Journal of Engineering, 10*, 33–38.
24. Paulraj, K., Irudayaraj, V., Johnson, M., & Patric, D. (2011). Phytochemical and anti-bacterial activity of epidermal glands extract of Christella parasitica (L.) H Lev. *Asian Pacific Journal of Tropical Biomedicine, 1*, 8–11.
25. Kumar A, Rohini Kanwar, and Surinder K. Mehta. Eucalyptus Oil-Based Nanoemulsion: A Potent Green Nanowagon for Controlled Delivery of Emamectin Benzoate, *ACS Agricultural Science & Technology* 2021 *1* (2), 76–88
26. Swamy MK, Akhtar MS, Sinniah UR. (2016). Antimicrobial Properties of Plant Essential Oils against Human Pathogens and Their Mode of Action: An Updated Review", Evidence-Based Complementary and Alternative Medicine, Article ID 3012462, 21. (2016)
27. Moradi, S., & Barati, A. (2019). Essential Oils Nanoemulsions: Preparation, Characterization and Study of Antibacterial Activity against Escherichia Coli. *International Journal of Nanoscience and Nanotechnology, 15*, 199–210.
28. John, T. M., Jacob, C. N., & Kontoyiannis, D. P. (2021). When Uncontrolled Diabetes Mellitus and Severe COVID-19 Converge: The Perfect Storm for Mucormycosis. *Journal of Fungi (Basel)., 15*(7), 298.
29. Rabagliati, R., Rodríguez, N., Núñez, C., Huete, A., Bravo, S., & Garcia, P. (2021). COVID-19-Associated Mold Infection in Critically Ill Patients. *Chile. Emerging Infectious Disease, 27*, 1454–1456.
30. D'agostino, M., Tesse, N., Frippiat, J. P., Machouart, M., & Debourgogne, A. (2019). Essential Oils and Their Natural Active Compounds Presenting Antifungal Properties. *Molecules, 24*(20), 3713.

31. Gao T, Zhou H, Zhou W, Hu L, Chen J, Shi Z. (2016). The Fungicidal Activity of Thymol against Fusarium graminearum via Inducing Lipid Peroxidation and Disrupting Ergosterol Biosynthesis. Molecules. 18; 21(6).
32. Singh, S., Fatima, Z., & Hameed, S. (2016). Insights into the mode of action of anticandidal herbal monoterpenoid geraniol reveal disruption of multiple MDR mechanisms and virulence attributes in Candida albicans. *Archives of Microbiology, 198*(5), 459–472.
33. Wen-Chien, Lu., Huang, D.-W., Chiun-C, R., Wang, C.-H., Tsai, J.-C., Huang, Y.-T., & Li, P.-H. (2018). Preparation, characterization, and antimicrobial activity of nanoemulsions incorporating citral essential oil. *Journal of Food and Drug Analysis, 26*, 82–89.
34. Jena, S., & Das, H. (2006). Modeling of particle size distribution of sonicated coconut milk emulsion: Effect of emulsifiers and sonication time. *Food Research International, 39*, 606–611.
35. Laxmi, M., Bhardwaj, A., Mehta, S., & Mehta, A. (2015). Development and characterization of nanoemulsion as carrier for the enhancement of bioavailability of artemether. *Artificial Cells Nanomedicine Biotechnology, 43*(5), 334–344.
36. Mccue, P., Kwon, Y. I., & Shetty, K. (2005). Anti-amylase, anti-glucosidase and anti-angiotensin I-converting enzyme potential of selected foods. *Journal of Food Biochemistry, 29*, 278–294.
37. Kwon, Y. I., Apostolidis, E., & Shetty, K. (2007). Evaluation of pepper (*Capsicum annuum*) for management of diabetes and hypertension. *Journal of Food Biochemistry, 31*, 370–385.